Motion control of wheel-legged robots: theoretical and experimental validation

He Xiao[1, a*]
[1] College of Electrical Information, Southwest Petroleum University, Nanchong City, Sichuan Province, China
*e-mail: [a]2380876169@qq.com

Junqi Sun[2, b]
[2] College of Electromechanical Engineering, Southwest Petroleum University, Nanchong City, Sichuan Province, China
[b]e-mail: 2768838565@qq.com

Haopan Fang[3, c]
[3] College of Electrical Information, Southwest Petroleum University, Nanchong City, Sichuan Province, China
[c]e-mail: 2923121227@qq.com

Xuan Wu[4, d]
[4] College of Computer Software, Southwest Petroleum University, Nanchong City, Sichuan Province, China
[d]e-mail: 3129835204@qq.com

Abstract: **This research paper is devoted to the study of the balancing motion of wheel-legged robots. By constructing a wheel-legged platform and modeling the dynamics based on physical mechanics, a linear control equation describing the characteristics of this system is finally derived from the nonlinear control equation. The LQR gain matrix as well as the leg length fitting function were derived using MATLAB mathematical operations. A linear quadratic regulator (LQR) and proportional-integral-derivative (PID) based controller is designed and implemented for deployment on an embedded control system. A series of real-world tests show that the wheel-leg platform can effectively maintain equilibrium in a variety of situations and has the ability to carry certain additional loads, demonstrating its potential application value and scalability.**

Keywords: Wheel-legged robot; Balance control; Balance experiment

I. INTRODUCTION

Wheeled-legged robots[1], as a class of innovative robotic platforms that combine the advantages of wheeled and legged mobility, demonstrate significant advantages in terrain adaptability, flexibility, energy efficiency, and versatility[2]. Compared with traditional four-wheeled mobile robots[3], which usually require a flat ground and less terrain with large height differences like steps, wheeled-legged robots are better able to adapt to complex and changing environments. In recent years, with the rapid development of mobile robot technology, research results from various countries have been published, such as the Ascento robot from ETH Zurich, the ANYmal quadruped robot from Switzerland[4], as well as the quadruped robot W1 from China's LimX Dynamics, and the wheel-legged robot Ollie from Tencent, which have all demonstrated to varying degrees the ability of wheel-legged robots to handle diverse terrains well.

Compared to traditional four-wheeled mobile robots, wheeled robots are not only able to travel at high speeds with low power consumption on flat surfaces, but also show high maneuverability when facing complex terrain[5]. However, ensuring that wheel-legged robots can maintain a stable balance in various environments is still a key technical challenge that needs to be solved. Therefore, the focus of this paper is on how to address the challenge of balancing in multiple terrains by building controllers to enhance the balancing ability of wheel-legged robots in different situations[6].

This research paper adopts a hybrid control scheme based on linear quadratic regulator (LQR) and feed-forward + proportional-integral-differential (PID), aiming to increase the robustness of the system on the basis of guaranteeing the balance of the robot. In addition, the mechanical design draws on the parallel five-bar wheel-leg structure used by Tencent's Ollie[7], and this mechanical design not only enhances the robot's balance stability in dynamic environments, but also reduces the difficulty of integrated control and improves the reliability of the system. This paper also introduces virtual model control (VMC) to further optimize the control performance and simplify the control difficulty, aiming at combining the advantages of LQR and PID control to achieve finer dynamic balance adjustment for wheel-legged robots.

In summary, the core objective of this research paper is to build a wheel-leg platform to conduct experiments in different working environments by establishing LQR, PID integrated controller and parallel five-bar wheel-leg structure, to verify the balance of the wheel-leg platform, and to lay the foundation for it to be able to carry out extended work[8].

II. KINEMATICS OF ROBOTS (DYNAMIC MODEL)

In order to simplify the control algorithms for robot balance and movement, this paper focuses on the motion characteristics of the wheel-leg platform, leg attitude, and drive wheel. Through the virtual model control (VMC) method, the five-link structure is simplified to a virtual leg, which is the straight-line segment from the midpoint of the line connecting the centers of the two hip joint motor rotor axes to the center of the drive wheel motor rotor axis. In this simplified model, the variation of the leg length is ignored and only the angular relationship between the virtual leg and the drive wheel axis with respect to the inertial reference system is considered. A more concise and effective integrated controller is finally designed to better realize the balance and movement of wheel-legged robots in different terrain conditions. The overall structure of the robot is shown in Figure 1.

2024 11th International Forum on Electrical Engineering and Automation (IFEEA) | 979-8-3315-1661-1/24/$31.00 ©2024 IEEE | DOI: 10.1109/IFEEA64237.2024.10878627

Figure 1 Robot overall

A. System modeling

By establishing a physical model (similar to an inverted pendulum model), it is divided into three parts: the body, the virtual leg, and the drive wheel. This creates the wheeled-leg inverted pendulum model shown in Figure 2.

The model parameters and their variables are listed in Tables 1 and 2.

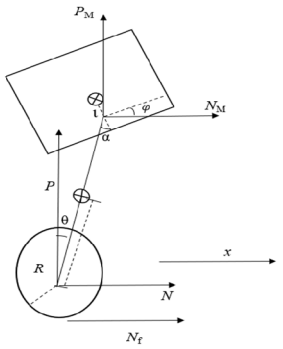

Figure 2 Wheel leg inverted pendulum model

TABLE 1 WHEEL-LEG INVERTED PENDULUM MODEL VARIABLE DEFINITION

Symbol	Meaning	Positive direction	Unit
F	Swing bar thrust	It's going to be positive	N
N	The horizontal component of the drive wheelset swing bar force	As shown by the arrow	N
P	The vertical component of the drive wheel to swing bar force	As shown by the arrow	N
N_f	Friction between the ground and the driving wheel	As shown by the arrow	N
N_M	Horizontal component of swing rod force on machine	As shown by the arrow	N
P_M	The vertical component of the swing rod force on the machine	As shown by the arrow	N
θ	Angle between swing bar and vertical direction	The figure shows the positive direction	rad
α	Relative Angle of swing rod and body	The figure shows the positive direction	rad
φ	Angle between body and horizontal	The figure shows the positive direction	rad
x	Drive wheel displacement	As shown by the arrow	m
x_b	Leg mechanism rotation axis displacement	Same as x	m
T	Drive wheel output torque	Same as θ	N·m
T_p	Hip joint output torque	Same as α	N·m

TABLE 2 MODEL PARAMETER DEFINITION OF WHEEL-LEG INVERTED PENDULUM

Symbol	unit	Meaning
R	m	Drive wheel radius
L	m	Distance between the center of gravity of the swing rod and the drive wheel shaft
L_M	m	The distance between the center of gravity of the pendulum rod and the rotating axis of the body
l	m	Distance from the center of gravity of the body to its axis of rotation
M_W	kg	Drive wheel rotor mass
M_P	kg	Mass of swing bar
M	kg	Mass of body
I_W	Kg·m^2	Moment of inertia of drive wheel rotor
I_p	Kg·m^2	Moment of inertia of the swing rod around the center of mass
I_M	Kg·m^2	Moment of inertia of the body around the center of mass

B. Mechanical analysis

Focus on the horizontal balance of the wheel-legged inverted pendulum. Perform a mechanical analysis of the body in the horizontal, vertical, and rotational directions:

$$N_{\mathrm{M}} = M(\ddot{\theta}_{\mathrm{b}} + l\varphi^2 \sin\varphi - l\ddot{\varphi}\cos\varphi) \tag{1}$$

$$P_{\mathrm{M}} - M\varrho = M\frac{\partial^2}{\partial t^2}\left((L + L_{\mathrm{M}})\cos\theta + l\cos\theta\right) \tag{2}$$

$$I_{\mathrm{m}}\ddot{\varphi} = T_{\mathrm{p}} + N_{\mathrm{M}} l\cos\varphi + P_{\mathrm{M}} l\sin\varphi \tag{3}$$

Perform a mechanical analysis of the virtual leg in the horizontal, vertical, and rotational directions:

$$N - N_M = m_p \frac{\partial^2}{\partial t^2}(x + L\sin\theta) \tag{4}$$

$$P - P_M - m_p g = m_p \frac{\partial^2}{\partial t^2}(L\cos\theta) \tag{5}$$

$$I_{\mathrm{p}}\ddot{\theta} = (PL + P_{\mathrm{M}} L_{\mathrm{M}})\sin\theta - (NL + N_{\mathrm{M}} L_{\mathrm{M}})\cos\theta - T + T_{\mathrm{P}} \tag{6}$$

Perform a mechanical analysis of the drive wheel in the horizontal and rotational directions:

$$N_{\mathrm{f}} - N = m_{\mathrm{w}}\ddot{x} \tag{7}$$

$$T - N_{\mathrm{f}} R = I_{\mathrm{w}}\frac{\ddot{x}}{R} \tag{8}$$

By combining Equation (7) with Equation (8), we obtain:

$$\ddot{x} = \frac{T - NR}{\frac{I_{\mathrm{w}}}{R} + m_{\mathrm{w}} R} \tag{9}$$

C. State-space equations

Establish the nonlinear state space equation:

$$\dot{x} = f(x,u) \tag{10}$$

Using the relevant tools, the above physical equations are solved to finally obtain the symbolic expression of the nonlinear model of the system. The state vector x and control vector u are respectively:

$$x = [\theta \quad \dot{\theta} \quad x \quad \dot{x} \quad \phi \quad \dot{\phi}]^T \; u = [T \quad T_p]^T \tag{11}$$

Solve the Jacobi matrix at the equilibrium point (the equilibrium point is the solution of $f(x, u)=0$) and linearize it.

$$\dot{\mathbf{x}} = \begin{bmatrix} 0 & 1 & 0 & 0 & 0 & 0 \\ A_1 & 0 & 0 & 0 & A_2 & 0 \\ 0 & 0 & 0 & 1 & 0 & 0 \\ A_3 & 0 & 0 & 0 & A_4 & 0 \\ 0 & 0 & 0 & 0 & 0 & 1 \\ A_5 & 0 & 0 & 0 & A_6 & 0 \end{bmatrix} \mathbf{x} + \begin{bmatrix} 0 & 0 \\ B_1 & B_2 \\ 0 & 0 \\ B_3 & B_4 \\ 0 & 0 \\ B_5 & B_6 \end{bmatrix} \mathbf{u} \quad (12)$$

After bringing in the model parameters to determine the state space matrix A and the control matrix B, the controllability matrix Co is judged and finally the full rank indicates that the system is controllable.

III. Design of robot control algorithms

A. Leg length control

Using the Virtual Model Control (VMC) algorithm, a unilateral wheeled-leg coordinate system is established to determine the virtual leg length L_{state} and the angle φ_0 , The error value $e = L_{set} - L_{state}$ is then fed into a feedforward + PD controller with K_p=170, K_d=80, feed-forward coefficient 22, to generate a holding torque F along the leg length. This torque helps maintain a consistent virtual leg length across various states.

B. Roll angle compensation

In order to make the wheel leg of the robot better shock absorption, prevent the occurrence of rapid reaction to the error, which causes the body to fall on its side and other situations, and the small Kp parameter in the feedforward +PD controller cannot well overcome the external disturbance. Therefore, a roll angle compensation K controller is added in series after the feedforward + PD controller. The roll angle compensation thrust is then superimposed on the moments F of the left and right wheel legs with opposite signs, which ultimately achieves the balance of the machine in a variety of terrains.

C. Balance of body

Based on the wheel-legged inverted pendulum model, the LQR controller is used, where the Q-weight matrix [1 1 100 50 300 1] and R-weight matrix [1 1], and finally the $K_{2\times6}$ feedback gain matrix is derived from the MATLAB calculation tool. In order to quickly obtain $K_{2\times6}$ under the current virtual leg length on the embedded platform, the fitting function $K_{ij}(L_0) = p_{0|ij} + p_{1|ij}L_0 + p_{2|ij}L_0^2 + p_{3|ij}L_0^3$ is obtained by using the MATLAB tool.

The average leg length is obtained from the left and right wheel leg coordinate system brought to the fitting function, fitted to $K_{2\times6}$, and then set:

$$\mathbf{x}_{set} = [0 \quad 0 \quad 0 \quad \dot{x}_b \quad 0 \quad 0]^T \quad (13)$$

And $u = K_{2\times6} \cdot (x_{set} - x_{state})$ to obtain $u = \begin{bmatrix} T & T_p \end{bmatrix}^T$, where T is the drive wheel output moment and T_p is the horizontal moment on the virtual leg, which together with the virtual leg thrust along the leg constitutes $F = \begin{bmatrix} F & T_p \end{bmatrix}^T$. According to the principle of virtual work, F combined with the Jacobi transpose matrix to calculate $T_A = J^T F$

$T_A = [T_1 \; T_2]^T$ is a matrix consisting of the output moments of the front and rear hip motors.

D. Steering of body

The LQR control quantities in this paper do not include the yaw angle. In the ideal case, the body is able to move forward in a coordinated manner. In general, the robot will be due to the structure of the body and other issues may greatly cause the left and right drive wheel speed inconsistency, so that the yaw angle is not closed-loop thus leading to the yaw angle dispersion, the body rotates horizontally. According to the difference between the desired yaw angle and the yaw angle obtained by IMU, the yaw correcting moment is obtained by the PD controller, which is eventually superimposed on T. The yaw stabilization can be achieved and can be stabilized. Yaw stabilization can be achieved and the steering can be stabilized.

E. Coordination of legs

In the steering control, the difference of the output torque of the two-legged drive wheels will produce a moment along the contact ground normal to the airframe, and this moment will make the difference between the angle of the left and right drive wheels wider and wider, resulting in splitting, and the system mismatch and thus divergence. To overcome this, a PD controller is used and $\theta_{error} = \theta_l - \theta_r$ is put into this controller to get a moment output that keeps the driving wheel pinch angle consistent. This pinch angle maintaining moment is superimposed on the Tp of the left and right wheel legs respectively with opposite sign.

F. Anti-skid

When the robot slips, it appears that the drive wheel speed is extremely fast. Data fusion of the body speed obtained from IMU, and the drive wheel speed is performed to obtain the overall speed of the body. When the body slips, even though the drive wheel speed is abnormal, the overall speed is normal, the LQR output is not affected, and the wheel-legged robot maintains balance.

G. Off ground detection

When the robot is off the ground with two wheels, the integrated control system is unable to allow the robot to maintain attitude stabilization in the air. Off-ground detection is the robot support force solving, which turns off the drive torque when off-ground occurs and maintains equilibrium. Conventional inverted pendulums have no vertical component and jumps are judged using multiple stages. When jumping, the robot drives the output of the hip joint motor to make the leg length quickly extend and stomp to vacate; after vacating, the leg is retracted and enters the off-ground detection to maintain balance; When landing, the PID+feedforward controller output for leg length retention compensates for leg length, exits off-ground detection, and quickly adjusts attitude.

Combining the above control algorithms, the final synthesized algorithm is constructed as shown in Figure 3.

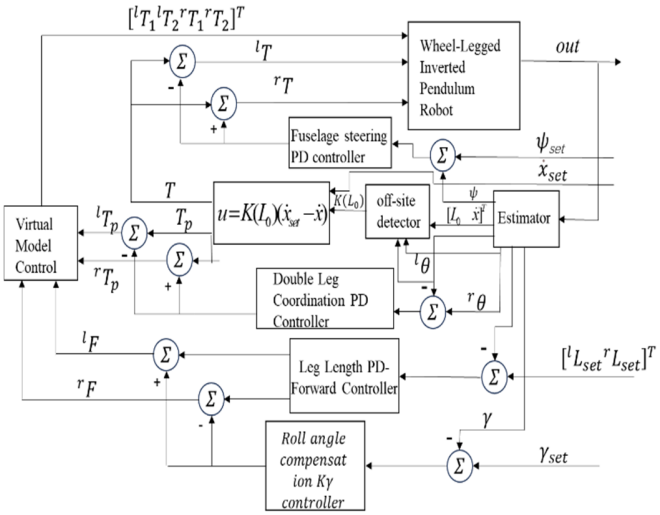

Figure 3 Block diagram of robot integrated motion control system

IV. Experimental Analysis Of Wheel-Legged Robots

The experimental data waveforms were collected through the relevant platforms with an acquisition interval of 10ms.

Startup Self-Balance: After the robot is started after being rested on the ground, and the positional behavior is shown in Figure 4, and φ, θ, $\dot{x}$ state changes are shown in Figure 5.

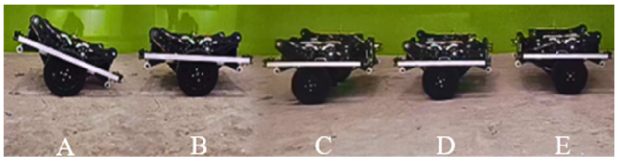

Figure 4 The lower pose performance is initiated by resting

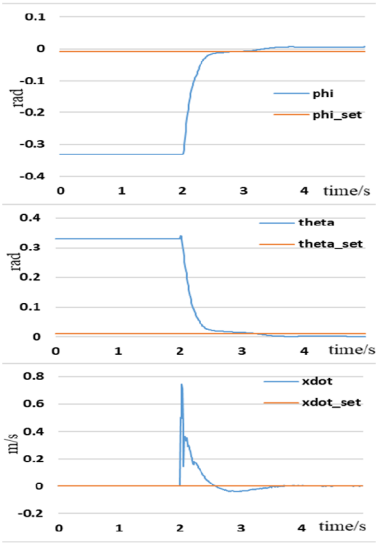

Figure 5 Pose graph after starting

It can be seen that when the robot is started, the robot can quickly make the motor output the specified torque through the LQR+PID fusion synthesis algorithm, so that the state quantity reaches the set amount, realizing that the machine body quickly reaches the equilibrium state from the state of falling to the ground, and realizing the startup self-balancing.

Balance Under External Disturbances: A short-time impact simulation perturbation is generated in the horizontal direction of the robot, and the posture performance is shown in Figure 6, and φ, θ, $\dot{x}$ state changes are shown in Figure 7.

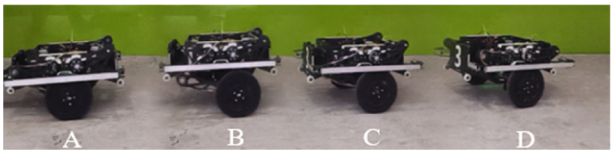

Figure 6 Interference with lower pose performance

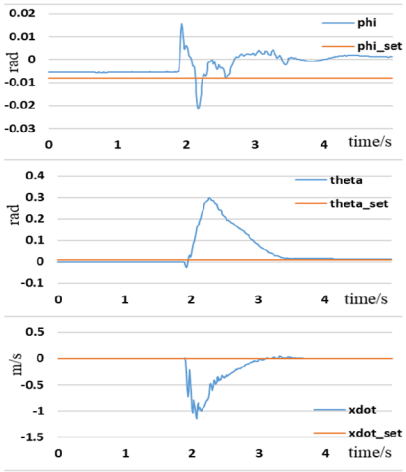

Figure 7 The pose curve after perturbation

It can be seen from the postural performance that the robot can also balance the upper body by adjusting the leg posture under external perturbation. Analyzed from the image, after the robot is subjected to external disturbances, the robot reacts quickly and the algorithm adjusts the pitch angle and the driving wheel angle to offset the external disturbances and finally stabilizes.

Balance While Moving: the robot's motion is realized by changing the expectation of $\dot{x}$. No matter in accelerated motion, uniform motion and steering motion, the body always maintains the balance of the body by adjusting each state quantity.

The performance of the emergency stops position posture and the change of φ, θ, $\dot{x}$ states after 2 s of motion at a set forward speed of 1 m/s are as shown in figures 8 and 9.

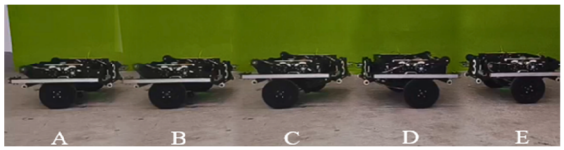

Figure 8 Pose representation in motion

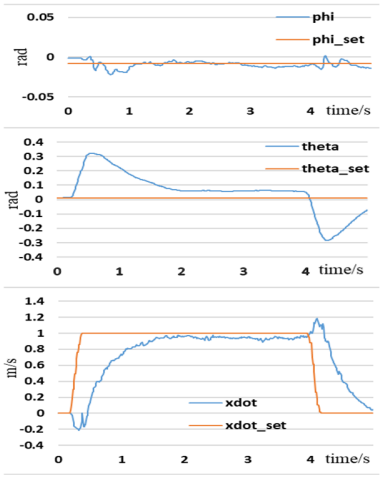

Figure 9 Pose curve during movement

It can be seen that the acceleration and deceleration are realized by adjusting the leg posture to generate a horizontal component force, and the pitch angle φ of the robot remains around the set -0.01rad during the whole movement process, which indicates that the algorithm is able to ensure the acceleration performance of the robot while taking into account the body posture.

Balance on Complex Terrains: In the face of various complex terrains, the wheel-legged robot is able to maintain the balance of the body through various terrains by controlling the leg length and compensating for the roll angle, and preventing skidding by fusing the velocity data. The position of the robot when passing through the irregular smooth road surface is shown in Figure 10.

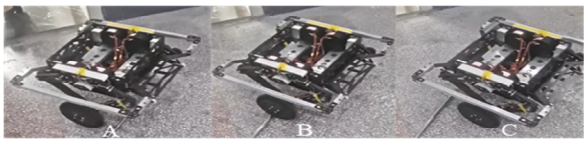

Figure 10 Pose performance during skid

Balance During Flying Slope and Jumping: The robot through the off-ground detection, in the air can still stabilize the attitude, in the instant of landing to adjust the attitude to maintain the balance of the whole process. The flying slope position is shown in Figure 11 as well as the jumping position in Figure 12.

Figure 11 Pose performance when flying slope

Figure 12 Pose performance while jumping

V. Conclusion

This research paper realizes most of the functions of the robot through LQR+PID fusion algorithm. Experiments verify that in most cases, the wheel-legged robot can maintain a high body balance to complete its work. This successfully verifies the obstacle-crossing ability and overall performance of the wheel-legged robot. However, relying solely on LQR+PID control, the robustness of the system is generally. For example, the maximum torque of the leg hip motors and leg drive wheel motors cannot reach the LQR torque output will lead to system dispersion, which can be improved by introducing the MPC model prediction for attitude correction and using the arithmetic board with the microcontroller[9]. The off-ground detection algorithm is used to realize the off-ground balance of the robot, but the off-ground algorithm judges the error in the harsh situation, and machine learning algorithms such as KNN can be used to improve the off-ground judgment. Through continuous optimization, wheel-legged robots are made more promising for a wider range of applications.[10].

Acknowledgment

Research presented in this paper was funded by Nanchong science and technology plan project(Grant No. 23YYJCYJ0066), Sichuan University Student Innovation and Entrepreneurship Project(Grant No. S202310615144 and S202310615164).

References

[1] Liu, X., Sun, Y., Wen, S., Cao, K., Qi, Q., Zhang, X., ... & Ji, A. (2024). Development of Wheel-Legged Biped Robots: A Review. Journal of Bionic Engineering, 21(2), 607-634.

[2] Rubio, F., Valero, F., & Llopis-Albert, C. (2019). A review of mobile robots: Concepts, methods, theoretical framework, and applications. International Journal of Advanced Robotic Systems, 16(2), 1729881419839596

[3] Song, S., Qu, J., Li, Y., Zhou, W., & Guo, K. (2016). Fuzzy control method for a steering system consisting of a four-wheel individual steering and four-wheel individual drive electric chassis. Journal of Intelligent & Fuzzy Systems, 31(6), 2941-2948.

[4] Bjelonic, M., Bellicoso, C. D., de Viragh, Y., Sako, D., Tresoldi, F. D., Jenelten, F., & Hutter, M. (2019). Keep rollin'—whole-body motion control and planning for wheeled quadrupedal robots. IEEE Robotics and Automation Letters, 4(2), 2116-2123.

[5] Mertyüz, İ., Tanyıldızı, A. K., Taşar, B., Tatar, A. B., & Yakut, O. (2020). FUHAR: A transformable wheel-legged hybrid mobile robot. Robotics and Autonomous Systems, 133, 103627.

[6] Bjelonic, M., Sankar, P. K., Bellicoso, C. D., Vallery, H., & Hutter, M. (2020). Rolling in the deep–hybrid locomotion for wheeled-legged robots using online trajectory optimization. IEEE Robotics and Automation Letters, 5(2), 3626-3633.

[7] Zhang, J., Li, Z., Wang, S., Dai, Y., Zhang, R., Lai, J., ... & Zheng, Y. (2023). Adaptive optimal output regulation for wheel-legged robot Ollie: A data-driven approach. Frontiers in Neurorobotics, 16, 1102259.

[8] Klemm, V., Morra, A., Gulich, L., Mannhart, D., Rohr, D., Kamel, M., ... & Siegwart, R. (2020). LQR-assisted whole-body control of a wheeled bipedal robot with kinematic loops. IEEE Robotics and Automation Letters, 5(2), 3745-3752.

[9] Pan, Z., Li, B., Zhou, S., Liu, S., Niu, Z., & Wang, R. (2023). Distributed MPC-based posture control for knee-wheeled wheel-legged robots with multi-actuation. Proceedings of the Institution of Mechanical Engineers, Part D: Journal of Automobile Engineering, 09544070231198901.

[10] Li, J., Wang, J., Peng, H., Hu, Y., & Su, H. (2021). Fuzzy-torque approximation-enhanced sliding mode control for lateral stability of mobile robot. IEEE Transactions on Systems, Man, and Cybernetics: Systems, 52(4), 2491-2500.